



New theoretical insight into indirect photochemical transformation of fragrance nitro-musks: Mechanisms, eco-toxicity and health effects

Yanpeng Gao^{a,b}, Guiying Li^a, Yaxin Qin^a, Yuemeng Ji^a, Bixian Mai^b, Taicheng An^{a,*}

^a Guangzhou Key Laboratory of Environmental Catalysis and Pollution Control, Guangdong Key Laboratory of Environmental Catalysis and Health Risk Control, School of Environmental Science and Engineering, Institute of Environmental Health and Pollution Control, Guangdong University of Technology, Guangzhou 510006, China

^b State Key Laboratory of Organic Geochemistry and Guangdong Key Laboratory of Environmental Resources Utilization and Protection, Guangzhou Institute of Geochemistry, Chinese Academy of Sciences, Guangzhou 510640, China



ARTICLE INFO

Handling Editor: Thanh Nguyen

Keywords:

Nitro-musks
Transformation mechanism
Hydroxyl radical
Carcinogenic activity
Theoretical calculation
Computational toxicology

ABSTRACT

The ubiquitous presence of fragrance-associated synthetic musk is cause for serious concern due to their transformation and environmental impacts. In particular, nitro-musks are frequently detected in various matrices, including water, even though they were restricted because of carcinogenicity. Thus, using musk xylene as a model compound, the mechanism, eco-toxicity and health effects during ·OH-initiated transformation process were systematically studied using quantum chemistry and computational toxicology. Results indicate that musk xylene can be exclusively transformed via H-abstraction pathways from its methyl group, with total rate constants of 5.65×10^8 – $8.79 \times 10^9 \text{ M}^{-1} \text{ s}^{-1}$, while the contribution of other pathways, including single-electron transfer and ·OH-addition pathways, were insignificant. The subsequent dehydrogenation intermediates (·MX (–H)) could further transform into cyclic, aldehyde and demethylation products. Based on toxicity assessments, all the transformation products exhibited decreased aquatic toxicity to fish in comparison with the parent musk xylene but they were still classified at toxic or very toxic levels, especially the cyclic products. More importantly, these products still exhibited carcinogenic activity during ·OH-initiated transformation and increased carcinogenicity relative to the parent musk xylene. This is the first time that the transformation mechanism and environmental impacts of nitro-musks have been explored through theoretical calculations.

1. Introduction

Synthetic musks have attracted extensive attention due to their widespread occurrence and eco-toxicological effects (Gao et al., 2017; Salvito, 2005). These compounds are extensively used as fragrances in various personal care products such as cosmetics, perfuming agents, toiletries, soaps and household cleaners. Nitro- and polycyclic musks are two common and important synthetic musks currently in use (Hopkins and Blaney, 2016). Particularly, nitro-musks were first developed as cheaper alternatives to natural musks and have been in use the longest. In the 1980s, nitro-musks were detected in environmental samples and aquatic organisms in Japan, triggering concerns about these chemicals (Yamagishi et al., 1981). Previous research has reported that nitro-musks could raise the possibility of exposure risks and xenobiotic accumulation in cells by inhibiting their normal exclusion (Luckenbach and Epel, 2005). In addition, because of their strong photochemical toxicity (Karschuk et al., 2010), carcinogenicity (Zhang et al., 2017) and neurotoxic properties, as well as endocrine

dysfunction, nitro-musks (e.g. musk xylene), have been listed among the ‘Monitoring Chemical Substances’ in Japan and are restricted in the European Union (Nakata et al., 2015).

Nevertheless, nitro-musks are still prevalent with diverse concentration (Table S1) in various environmental matrices, including water (Liu and Wong, 2013; Zeng et al., 2018) and aquatic organisms (Kannan et al., 2005; Nakata et al., 2007; Ramirez et al., 2009; Wan et al., 2007). Moreover, they can concentrate in the food chain through bioaccumulation (Chen et al., 2015; Gatermann et al., 2002). Additionally, the high consumption in drinking water and fish, as well as using personal care and household products that contain nitro-musks, could result in serious exposure to humans. Accordingly, nitro-musks have also been detected frequently in human milk (Lignell et al., 2008; Reiner et al., 2007), adipose tissue and blood (Hutter et al., 2010; Hutter et al., 2009). More importantly, transformed products of nitro-musks have been observed in aquatic environments (Berset et al., 2000), sometimes at concentrations of up to 40 times more than those of the parent compounds (Rimkus et al., 1999). Thus, it is very

* Corresponding author.

E-mail address: ante99@gdut.edu.cn (T. An).

<https://doi.org/10.1016/j.envint.2019.05.020>

Received 1 January 2019; Received in revised form 6 May 2019; Accepted 8 May 2019

0160-4120/© 2019 The Authors. Published by Elsevier Ltd. This is an open access article under the CC BY-NC-ND license (<http://creativecommons.org/licenses/by-nc-nd/4.0/>).

important to understand the environmental transformation and fate of nitro-musks in aquatic environments, as well as the adverse effects of these transformation products on aquatic ecosystems and human beings.

Nitro-musks, such as musk xylene, were found to be non-biodegradable under aerobic conditions (Tas et al., 1997). In contrast, they can undergo reduction reactions on their nitro groups under anaerobic conditions, leading to the formation of 2/4-amino-musk xylenes (Kafferlein et al., 1998). Besides biodegradation, the photochemical pathway including direct and indirect photolysis is both important transformation process for emerging organic contaminants (EOCs) in aquatic environments, for instance, natural water and advanced oxidation process (AOP) (An et al., 2014; Gao et al., 2019; Xiao et al., 2018); however, there is very limited information concerning the photochemical degradation behavior of nitro-musks. A few studies have reported on the photolysis of nitro-musks, and the results indicated that nitro-musks were photochemically degradable (Butte et al., 1999). For instance, above 80% of xylene musk could be photodegraded after 30 min of UV irradiation, and its apparent rate constant and half-life time were reported as 0.003 s^{-1} and 218 s, respectively (Sanchez-Prado et al., 2004). These data indicate that the direct photolysis also is very important for the environmental transformation of nitro-musks. Furthermore, this photochemical process was inhibited by the formation of photo-transformation products (Butte et al., 1999), suggesting that a similar inhibitory effect of dissolved organic matter (DOM) on the direct or indirect photo-transformation of nitro-musks could be observed (Janssen et al., 2014). Subsequent photocyclization, photoreduction and photorearrangement products were observed during the UV irradiation (Sanchez-Prado et al., 2004). It is well-known that these products can quench the photolabile excited state of intermediates, giving them reasonable ability to inhibit further transformation of the produced intermediates in the direct photolysis system. Moreover, several photoproducts are more persistent and stable than the parent nitro-musks such as musk tibetene and moskene during direct photolysis (Canterino et al., 2008).

Together with direct photolysis, indirect photochemical transformation of EOCs in aquatic environments could also likely occur due to the presence of various reactive species including $\cdot\text{OH}$. Accordingly, both of direct and indirect photolysis could impact the environmental fate of EOCs (Fenner et al., 2013). In addition, indirect photolysis of EOCs is dependent on the environmental parameters (e.g. concentration of sensitizers and reactive species, etc.). For instance, it was reported that the rate constant reached up to $1.30 \times 10^3 \text{ s}^{-1}$ for the photochemical degradation of xylene musk at a dose of $1.17 \mu\text{M H}_2\text{O}_2$ with high concentration of $\cdot\text{OH}$ (Neamtu et al., 2000). In fact, high concentration of $\cdot\text{OH}$ was reported in various AOPs (e.g. UV/ H_2O_2 system) (Neamtu et al., 2000; Sanchez-Prado et al., 2004) and even several surface waters such as collected from Lake Nichols, northern Wisconsin (Brezonik and Fulkerson-Brekken, 1998), and west-central Indiana that receive acidic mine drainage runoff (Allen et al., 1996). However, compared with the direct photolysis of nitro-musks, the indirect photochemical transformation is rarely focused. Thus, to comprehensively understand the fate of nitro-musks, indirect photochemical transformation is calculated on the mechanisms, environmental fate as well as transformation products of nitro-musks.

In silico analysis is a helpful approach to reveal the environmental behavior and transformation mechanisms of pollutants at molecular level (Gao et al., 2014a; Gao et al., 2015; Gao et al., 2014b; Hansel et al., 2014; Luo et al., 2018; Wang et al., 2011; Xiao et al., 2015). In this work, both quantum chemistry and computational toxicology were used to explore the mechanisms and environmental impacts of nitro-musks during indirect photochemical transformation. Musk xylene is of particular interest for three reasons: (a) musk xylene is still dominant in commercial products containing nitro-musks and frequently detected at high levels in aquatic environments; (b) the carcinogenic activity of musk xylene is noteworthy; and (c) the simple and symmetrical

molecular structure of musk xylene could reduce the cost of calculation. The transformation mechanisms, fate and kinetics of musk xylene during $\cdot\text{OH}$ -initiated indirect photolysis in aquatic environments were systematically elucidated. Additionally, the environmental persistence of musk xylene and its products are carefully discussed herein. Finally, the potential ecotoxicity and human carcinogenic risks of parental musk xylene and its products were assessed during $\cdot\text{OH}$ -initiated photochemical transformation. The findings could provide important information to better understand the environmental geochemistry of nitro-musks and to evaluate their potential risks to human health and aquatic organisms, especially with respect to the secondary pollution imposed by their photo-transformation products.

2. Computational methods

2.1. Quantum chemistry calculation

All quantum chemical calculations were carried out using the Gaussian 09 package (Frisch et al., 2009). The electronic structures and vibrational frequency for the parent musk xylene, as well as its transformation products and transition states (TSs) were calculated using the M06-2X method with the 6-31 + G(d,p) basis set (Zhao and Truhlar, 2008a, 2008b). M06-2X has been proven to be a reliable calculation for transformation mechanisms, kinetics and environmental fates of organic pollutants (Li et al., 2014; Zhao and Truhlar, 2008b). By comparison the reliability of different computational methods (Discussion in Supplementary materials), M06-2X with the lowest standard deviations tends to be closer to the experimental value (Table S2), further confirming the reliability of this method.

The recommended continuum solvation model SMD was employed to determine the effect of solvent water (Marenich et al., 2009). Using the intrinsic reaction coordinate (IRC) theory, every TS of the transformation pathway was further confirmed to indeed connect the reactants (musk xylene and $\cdot\text{OH}$) with the respective transformation product. Next, 6-311 + G(3df,2p), as a high-level basis set, was used to calculate energies, including the reaction energy (ΔG) and the energy barrier (ΔG^\ddagger), of all transformation pathways. Accordingly, the profile of the potential energy surface (PES) for $\cdot\text{OH}$ -initiated transformation of musk xylene was established at the M062X/6-311 + G(3df,2p) level. The calculation of the reaction kinetics was carried out using the transition-state theory (TST). The cage effect of solvent water was also considered to fully simulate realistic conditions in the aquatic environment.

2.2. Eco-toxicity and carcinogenicity evaluation

The eco-toxicity of musk xylene and its transformation products were evaluated using the ecological structure–activity relationships (ECOSAR) model (ECOSAR, 2014), which was established by the United States Environmental Protection Agency (US EPA). Fish were selected as the model aquatic species in this work, since they usually serve as food for human beings and other species. Acute toxicity during transformation of musk xylene was expressed by the median lethal concentration (LC_{50}) after 96-h exposure and the lowest effect concentrations were reported with conservative consideration under the precautionary principle. Carcinogenicity assessments of musk xylene and its transformation products were completed using the lazar (lazy structure–activity relationship) program (Maunz et al., 2013).

3. Results and discussion

3.1. Transformation mechanisms of musk xylene during the initial step

For the $\cdot\text{OH}$ -initiated reaction of musk xylene, all possible pathways were modeled in detail as illustrated in Fig. 1. That is, three different types of reaction mechanisms were fully considered: (i) H-abstraction

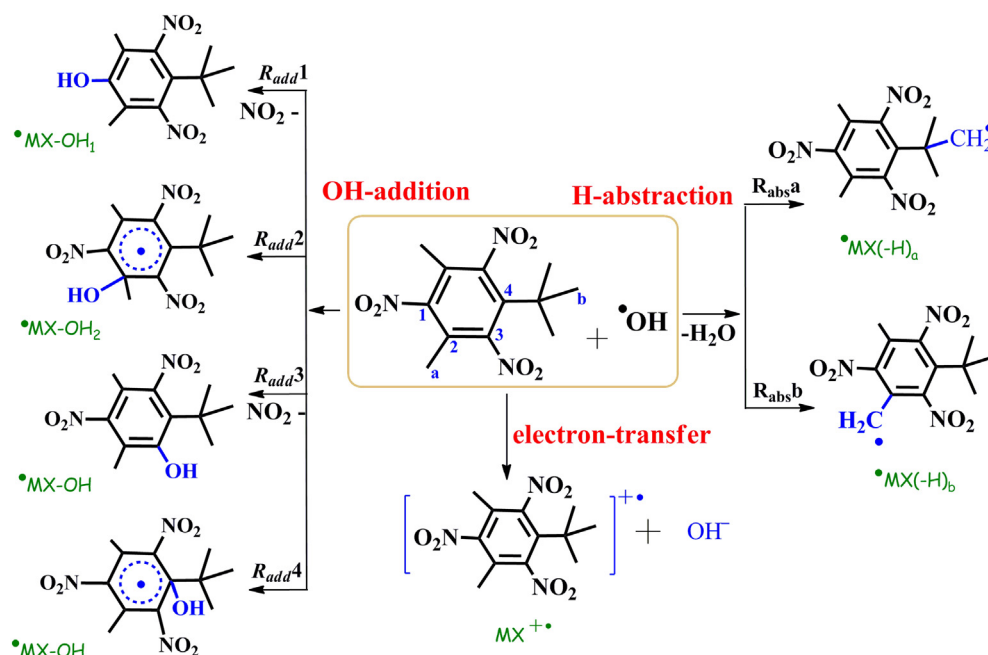


Fig. 1. All the reaction pathways in the initial reaction of musk xylene with $\cdot\text{OH}$.

from the methyl group of musk xylene (R_{absa} and R_{absb}); (ii) $\cdot\text{OH}$ -addition to the benzene ring of musk xylene (R_{add1-4}); and (iii) the single-electron transfer mechanism from the musk xylene molecule (R_{set}). This R_{set} pathway was an endothermic process with a reaction energy (ΔG^\ddagger) of $47.99 \text{ kcal mol}^{-1}$, implying that the R_{set} pathway is unlikely to occur from a thermodynamic standpoint and that musk xylene has a very low reactivity in the electron transfer mechanism. Furthermore, the energy barrier (ΔG^\ddagger) of the R_{set} pathway was calculated to be as high as $102.46 \text{ kcal mol}^{-1}$, further confirming that the electron transfer pathway is unlikely to occur during $\cdot\text{OH}$ -initiated transformation of musk xylene. This finding could probably be ascribed to the structural characteristic of musk xylene. That is, three nitro ($-\text{NO}_2$) groups in the musk xylene molecule have a strong electron-withdrawing inductive effect and a conjugation effect (Politzer et al., 1987). This could account for the low reactivity of the single electron transfer mechanism of musk xylene with $\cdot\text{OH}$; thus, the single-electron transfer pathway can be ruled out during the $\cdot\text{OH}$ -initiated indirect photochemical transformation step of musk xylene in the aquatic environment, although this mechanism is very important for other radical-initiated transformation of pollutants such as sulfate radical anion ($\text{SO}_4^{\cdot-}$) (Xiao et al., 2015). Therefore, the following discussion will focus on the other two reaction mechanisms, namely $\cdot\text{OH}$ -addition (R_{add1-4}) and H-abstraction (R_{absa} and R_{absb}).

The potential energy surface (PES) of the $\cdot\text{OH}$ -initiated transformation pathway of musk xylene is shown Fig. 2. It is clear that the reaction energy of these possible pathways, namely $\cdot\text{OH}$ -addition (R_{add1-4}) and H-abstraction (R_{absa} and R_{absb}), were negative ($-5.94 \sim -27.55 \text{ kcal mol}^{-1}$). The results imply that they are exothermic processes and that they potentially contribute to the transformation of musk xylene from the standpoint of thermodynamics. Among these pathways, H-abstraction (R_{absa} and R_{absb}) would release reaction energies of 27.55 and $23.47 \text{ kcal mol}^{-1}$, while $\cdot\text{OH}$ -addition (R_{add1-4}) would release less energy of $5.94\text{--}18.22 \text{ kcal mol}^{-1}$. These data suggest that the H-abstraction pathways are more thermodynamically favorable when compared with the $\cdot\text{OH}$ -addition pathways. Furthermore, the energy barrier of the R_{absa} and R_{absb} pathways were determined as 10.36 and $10.69 \text{ kcal mol}^{-1}$, respectively, which are $3.4\text{--}7.6 \text{ kcal mol}^{-1}$ lower than those of the $\cdot\text{OH}$ -addition pathways (R_{add1-4}). These results mean that the H-abstraction (R_{absa} and R_{absb}) pathways could be more kinetically favorable than the $\cdot\text{OH}$ -addition pathways. Therefore, the

R_{absa} and R_{absb} pathways were predicted as the main routes for $\cdot\text{OH}$ -initiated photochemical transformation of musk xylene in aquatic environment, producing the dehydrogenated radical intermediates $\cdot\text{MX}(-\text{H})_a$ and $\cdot\text{MX}(-\text{H})_b$.

3.2. Transformation kinetics and environmental persistence

To further confirm the main pathways and environmental fate during $\cdot\text{OH}$ -initiated indirect photochemical transformation of musk xylene in aquatic environments, it was necessary to quantitatively evaluate the contributions of all possible pathways. The reaction kinetics were calculated within a realistic temperature range (273–313 K) for aquatic environments. The rate constants of each pathway, including $\cdot\text{OH}$ -addition (R_{add1-4}) and H-abstraction (R_{absa} and R_{absb}), as well as the overall rate constants (k_{total}), are given in Table 1. The k_{total} was determined as $5.65 \times 10^8\text{--}8.79 \times 10^9 \text{ M}^{-1} \text{ s}^{-1}$, which was near the diffusion-controlled reaction ($4 \times 10^9 \text{ M}^{-1} \text{ s}^{-1}$) of the entire temperature range. These data suggest that photochemical transformation of musk xylene initiated with $\cdot\text{OH}$ is very quick and is mainly controlled by the diffusion of reactants (musk xylene and $\cdot\text{OH}$) in the aquatic environment. Furthermore, as the water temperatures increased, the rate constants of each pathway and the overall reaction during musk xylene transformation increased (Table 1). For instance, the rate constant for the H-abstraction pathway R_{absa} was 4.15×10^8 at 273 K, which was 15 times lower than that at 313 K ($6.31 \times 10^9 \text{ M}^{-1} \text{ s}^{-1}$). Therefore, it could be deduced that a high environmental temperature is beneficial for the transformation of musk xylene. Moreover, this finding could partly explain the experimental observation of an important seasonal distribution of synthetic musk in aquatic environments (Lange et al., 2015), together with the seasonality of the amount of UV light.

Furthermore, the contribution of each transformation pathway to the overall reaction is expressed as a branching ratio (Γ), which was obtained using the formula $\Gamma_i = \frac{k_i}{k_{total}}$, where k_i is the rate constant of the i th transformation pathway. The calculated Γ 's are summarized in Fig. 4. It is clear that the H-abstraction pathway (R_{absa}) was the predominant pathway, particularly with a Γ_{absa} of up to 73.4% at 273 K. Although the Γ_{absa} decreased to 71.7% with the environmental temperature increased to 313 K, it was still at least 43.0% higher than those

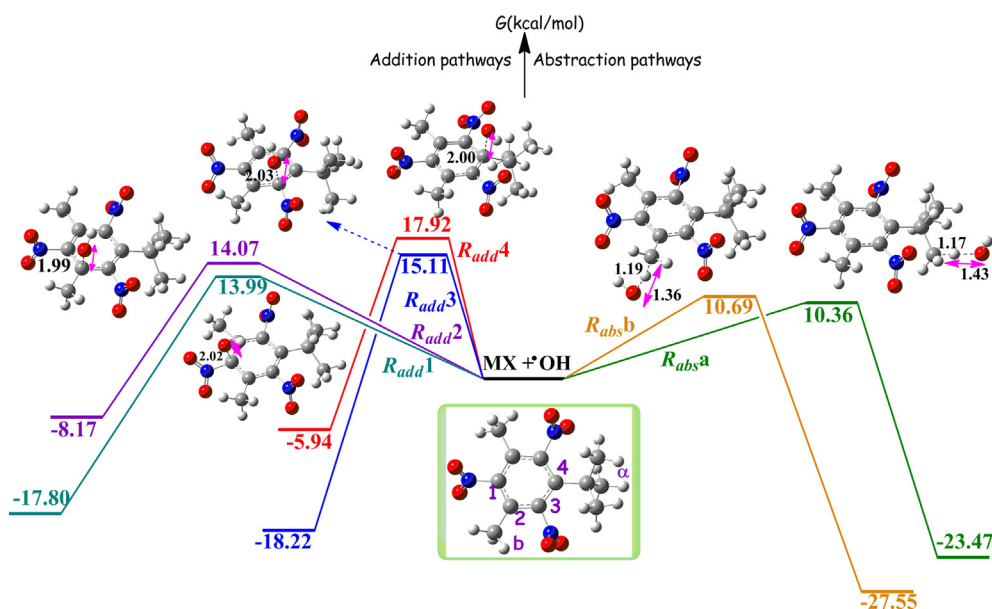


Fig. 2. Schematic diagram of free energy for the reaction of musk xylene with $\cdot\text{OH}$ at the M062X/6-311 + G(3df,2p)//M062X/6-31 + G(d,p) level, and all possible routes for the reactions of musk xylene with $\cdot\text{OH}$.

of the other H-abstraction pathway ($R_{\text{abs},b}$). As for the $\cdot\text{OH}$ -addition pathways ($R_{\text{add}1-4}$), the $\Gamma_{\text{add}1-4}$ were $< 0.1\%$ within the tested temperature range of the aquatic environment (273–313 K). These data suggest that the contribution of all $\cdot\text{OH}$ -addition pathways are negligible. For example, at 298 K, $\Gamma_{\text{add}1-4}$ were calculated as 0.03%, 0.06%, 0.01% and 0.00%, respectively, while $\Gamma_{\text{abs},a}$ and $\Gamma_{\text{abs},b}$ were 72.3% and 27.6%, respectively. This result is different with the transformation mechanism of polycyclic musk tonalide (Gao et al., 2016b), in which $\cdot\text{OH}$ -addition pathway was dominant at low temperature ($< \sim 287$ K). This indicates that the different functional groups on benzenic ring of musk could significantly affect the transformation pathways and products. Therefore, it is confirmed that both H-abstraction pathways, $R_{\text{abs},a}$ and $R_{\text{abs},b}$, were the dominant pathways of $\cdot\text{OH}$ -initiated photochemical transformation of musk xylene within the tested temperature range. Accordingly, the dehydrogenized intermediates, $\cdot\text{MX}(-\text{H})_a$ and $\cdot\text{MX}(-\text{H})_b$ (Fig. 2), were mainly formed.

Furthermore, the Arrhenius formula was fitted for each reaction pathway and for the overall transformation of musk xylene (Table S3) in order to provide important information regarding reaction kinetics, such as the activation energy, rate constant and pre-exponential factor. In this work, the activation energy was determined as $11.65 \text{ kcal mol}^{-1}$ for $\cdot\text{OH}$ -initiated photochemical transformation of musk xylene in aquatic environments. This is approximately 2.8 times higher than that of polycyclic musk tonalide ($4.11 \text{ kcal mol}^{-1}$), as determined in our previous work (Gao et al., 2016b). This finding implies that, compared with polycyclic musk, nitro-musk is less easily transformed, potentially leading to greater persistence.

To further explore the persistence of musk xylene during $\cdot\text{OH}$ -initiated photochemical transformation, its half-life ($t_{1/2}$) was calculated

using the formula $t_{1/2} = \ln 2 / (k_{\text{total}} \times [\cdot\text{OH}])$, where $[\cdot\text{OH}]$ is the concentration of $\cdot\text{OH}$. Generally, the $[\cdot\text{OH}]$ is approximately 10^{-15} – 10^{-18} M in surface water (Brezonik and Fulkerson-Brekken, 1998; Burns et al., 2012) and can be up to 10^{-12} – 10^{-14} M in lake water (Brezonik and Fulkerson-Brekken, 1998) and special aquatic environments, such as acid mine wastewater (Allen et al., 1996). As seen from Fig. 3, the half-life of musk xylene decreased from 38 y to 20 s as the $[\cdot\text{OH}]$ increased from 10^{-18} to 10^{-12} M within a temperature range of 273–313 K. In particular, at ambient temperatures (298 K), as the $[\cdot\text{OH}]$ decreased from 10^{-12} to 10^{-18} M, the $t_{1/2}$ increased from 3.39 min to 6.45 y. Moreover, at ambient temperatures, the $t_{1/2}$ was determined as 5.65 h for nitro-musk musk xylene, which is 3.6 times higher than that of polycyclic musk tonalide (1.59 h) in aquatic environments such as Lake Nichols, northern Wisconsin at the $\cdot\text{OH}$ concentration of 10^{-14} M (Brezonik and Fulkerson-Brekken, 1998; Gao et al., 2016b). These data could theoretically confirm the fact that from the respective of $\cdot\text{OH}$ -initiated photochemical transformation, nitro-musk, including musk xylene, is more persistent than polycyclic musk tonalide in aquatic environments, potentially leading to increased environmental risks.

Furthermore, based on the persistence guidelines specified by the Stockholm Convention (Klasmeier et al., 2005), a half-life of 60 d in aquatic environments is the threshold for persistent organic pollutant (POP)-like compounds. The half-life of musk xylene could exceed 60 d during $\cdot\text{OH}$ -initiated photochemical transformation in aquatic environments when the $\cdot\text{OH}$ concentration is below 2.37×10^{-16} – $1.52 \times 10^{-17} \text{ mol L}^{-1}$ at 273–313 K. Thus, the persistence of musk xylene and the related adverse effects deserve more attention.

Table 1

Calculated rate constants ($\text{M}^{-1} \text{ s}^{-1}$) between 273 and 313 K in the reaction of musk xylene and $\cdot\text{OH}$.

T (K)	273	283	293	298	303	313
$R_{\text{add}1}$	1.12×10^5	3.00×10^5	7.54×10^5	1.17×10^6	1.79×10^6	4.01×10^6
$R_{\text{add}2}$	1.93×10^5	5.20×10^5	1.31×10^6	2.04×10^6	3.13×10^6	7.05×10^6
$R_{\text{add}3}$	2.82×10^4	8.14×10^4	2.19×10^5	3.50×10^5	5.53×10^5	1.32×10^6
$R_{\text{add}4}$	78.1	2.71×10^2	8.63×10^2	1.50×10^3	2.56×10^3	7.08×10^3
$R_{\text{abs},a}$	4.15×10^8	8.77×10^8	1.77×10^9	2.47×10^9	3.40×10^9	6.31×10^9
$R_{\text{abs},b}$	1.50×10^8	3.25×10^8	6.67×10^8	9.40×10^8	1.31×10^9	2.47×10^9
k_{total}	5.65×10^8	1.20×10^9	2.44×10^9	3.41×10^9	4.72×10^9	8.79×10^9

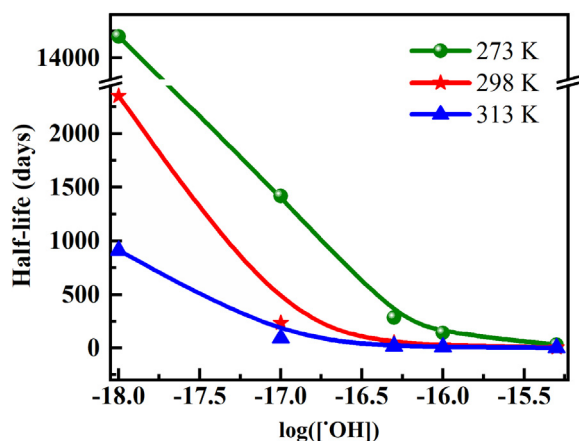


Fig. 3. In natural waters, calculated half-life ($t_{1/2}$) of musk xylene transformation as a function of $[\cdot\text{OH}]$ (unit: M) in temperature range of 273–313 K.

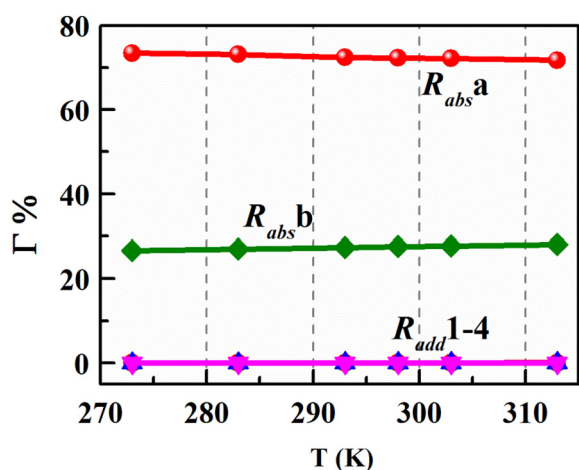


Fig. 4. Calculated branching ratio (Γ) of each route in the reaction of musk xylene with $\cdot\text{OH}$ at 273–313 K.

3.3. Primary transformation products

The main intermediates, $\cdot\text{MX}(-\text{H})_a$ and $\cdot\text{MX}(-\text{H})_b$, that are generated from the initial step of $\cdot\text{OH}$ -initiated photochemical transformation of musk xylene are highly reactive radicals that can continue to react to form stable intermediates. Thus, it is necessary to further trace the transformation of these radical intermediates. Fig. 5 depicts the transformation pathways of $\cdot\text{MX}(-\text{H})_a$. It can be seen that the energy barrier of the cyclization pathway was $7.48 \text{ kcal mol}^{-1}$, which is less than the energy released from the initial formation of $\cdot\text{MX}(-\text{H})_a$. This indicates that the cyclization pathway should easily occur to form the intermediate IM-Sa1. Furthermore, the intermediate IM-Sa1 can successively undergo H-transfer and a dehydroxylation reaction with a ΔG^\ddagger of 20.83 and $3.08 \text{ kcal mol}^{-1}$, respectively, thereby resulting in the formation of the cyclic product PC1a. A similar transformation pathway for $\cdot\text{MX}(-\text{H})_b$ was observed (Fig. S1), mainly forming the cyclic product PC1b. These transformation products were previously experimentally observed in aquatic environments (Butte et al., 1999; Sanchez-Prado et al., 2004). Furthermore, this finding reveals the formation mechanism of the cyclic products in detail during the indirect photochemical processes of musk xylene, together with direct photolysis. Additionally, this intramolecular process can accompany the formation of $\cdot\text{OH}$, which could also be involved in the subsequent musk xylene reaction.

The generated $\cdot\text{OH}$ could further attack these main intermediate radicals ($\cdot\text{MX}(-\text{H})_a$ and $\cdot\text{MX}(-\text{H})_b$) especially in $\cdot\text{OH}$ -enriched

environments, such as lakes, acid mine wastewater and advanced oxidation processes. The reactions of the intermediate radicals $\cdot\text{MX}(-\text{H})_a$ and $\cdot\text{MX}(-\text{H})_b$ with $\cdot\text{OH}$ were barrier-less processes, simultaneously releasing large reaction energies of 101.07 and $100.09 \text{ kcal mol}^{-1}$, respectively (Fig. 5 and S2). Furthermore, the released energy was much more than the energies required by the subsequent transformation (82.75 and $84.25 \text{ kcal mol}^{-1}$). Accordingly, the aldehyde product (PC2a; Fig. S5) and the demethylation product (PC2b; Fig. S2) were mainly formed from $\cdot\text{MX}(-\text{H})_a$ and $\cdot\text{MX}(-\text{H})_b$, respectively. Simultaneously, small molecular products, such as formaldehyde and methane, can be also generated.

For the purpose of fully identifying the environmental fate of musk xylene during $\cdot\text{OH}$ -initiated photochemical transformation in aerated water, the subsequent reactions of the intermediates were also considered in the presence of O_2 . $\cdot\text{MX}(-\text{H})_a$ could readily react with O_2 through an exothermic process with a ΔG of $43.50 \text{ kcal mol}^{-1}$ (Fig. 5), leading to the barrier-less formation of a peroxy intermediate ($\cdot\text{MX}-\text{OO}_a$). Meanwhile, the released energy could easily overcome the barrier ($41.28 \text{ kcal mol}^{-1}$) of the $\cdot\text{MX}-\text{OO}_a$ dehydroxylation reaction. As a result, the aldehyde product (PC3a) was generated accompanying the formation of $\cdot\text{OH}$. Similar results were observed during the transformation of $\cdot\text{MX}(-\text{H})_b$ intermediates (Figs. S3). That is, in aerated water, the $\cdot\text{MX}(-\text{H})_b$ intermediates were easily converted into the aldehyde product (PC3b) accompanying the formation of $\cdot\text{OH}$.

In brief, our theoretical results suggest that musk xylene can be readily attacked by a highly reactive $\cdot\text{OH}$ species in the aquatic environment and that two dehydrogenated radical intermediates, $\cdot\text{MX}(-\text{H})_a$ and $\cdot\text{MX}(-\text{H})_b$, were first formed via the H-abstraction pathways ($R_{abs}a$ and $R_{abs}b$). Furthermore, cyclic products (PC1a and PC1b), the demethylation product (PC2b) and aldehyde products (PC2a, PC3a and PC3b) were mainly formed accompanying the generation of $\cdot\text{OH}$, as were several small molecular products, such as formaldehyde and methane. Therefore, during $\cdot\text{OH}$ -initiated photochemical transformation of musk xylene both in AOPs systems and surface water, the ecological and health risks from these intermediates need to be seriously considered.

3.4. Aquatic toxicity of musk xylene and its transformation products

Computational toxicology as a promising and cost-effective approach is widely applied to predict environmental and health risks. Moreover, it can also avoid the use of animals during toxicity measurements, as well as supply adequate data for quick toxicity screening while supplementing experimental research. For instance, the ECOSAR program was successfully used as a reliable method to predict aquatic toxicities of emerging organic pollutants and their products (Butt et al., 2007; Gao et al., 2015; Gao et al., 2014b; Gao et al., 2016a). Thus, this study used the ECOSAR model to estimate the aquatic toxicity of musk xylene and its transformation intermediates (Table S4). The obtained LC_{50} of musk xylene was lower than 1.0 mg L^{-1} , which classifies it as a very toxic compound ($\text{LC}_{50} < 1.0 \text{ mg L}^{-1}$) in accordance with the aquatic toxicity criteria of the European Union (Table S5). Thus, musk xylene can exhibit high acute toxicity to fish. Similarly, musk xylene was identified as very chronically toxic towards fish because of its chronic toxicity value (ChV) of 0.01 mg L^{-1} . Therefore, it can be concluded that musk xylene possesses both acute and chronic toxicological effects and it can impose great negative impacts on aquatic organisms. Therefore, the aquatic toxicity of its products also deserves much attention.

The acute and chronic toxic values of cyclization pathway transformation products are shown in Table S4. The LC_{50} values for fish were determined as 0.89 and 0.50 mg L^{-1} for intermediates PC1a and PC1b, respectively, which are higher than that of musk xylene (0.20 mg L^{-1}). This indicates that their acute toxicity is lower than parent musk xylene; however, they are still regarded as very toxic. As for chronic toxicity during the cyclization pathways, the ChV values were

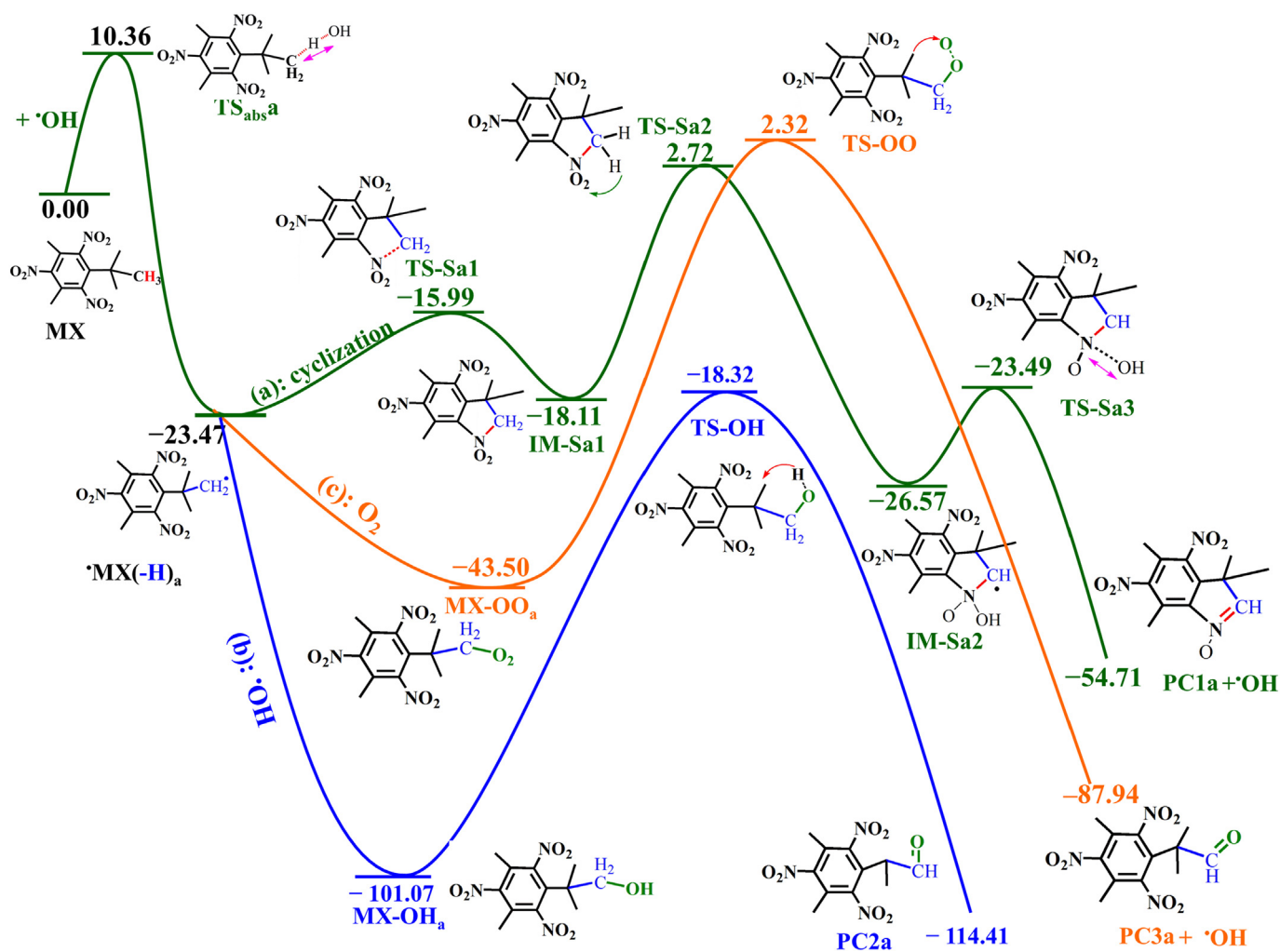


Fig. 5. Schematic diagram of the subsequent pathways of $\cdot\text{MX}(-\text{H})_a$. a: through cyclization process; b: with enough $\cdot\text{OH}$; c: with O_2 .

determined as 0.02 and 0.01 mg L^{-1} for intermediates PC1a and PC1b, respectively, which are around that of parent musk xylene (0.01 mg L^{-1}). Thus, conclude can be drawn that the chronic toxicity of the intermediates was nearly the same as the parent musk xylene.

An $\text{LC}_{50} > 1.0 \text{ mg L}^{-1}$ was obtained for all the transformation products (MX-OHa, MX-OHa, PC2a and PC2b) from the $R_{abs}a$ and $R_{abs}b$ pathways in the $\cdot\text{OH}$ -rich aquatic environment, except for PC2b, implying that all these intermediates were classified as toxic to fish; thus, the aquatic toxicity decreased as compared with parent musk xylene. However, intermediate PC2b ($\text{LC}_{50} = 0.44 \text{ mg L}^{-1}$) was found to be more toxic than the other intermediates and equally as toxic as the parent musk xylene.

In the aerated aquatic environment, O_2 participates in the subsequent transformation of musk xylene, leading to the formation of products PC3a and PC3b. Thus, the acute toxicity of product PC3a was classified as toxic due to its LC_{50} of 2.11 mg L^{-1} , implying that the acute toxicity of this pathway decreased by one toxicity level when compared with parent musk xylene. Although the LC_{50} of PC3b was 0.76 mg L^{-1} , which was higher than the parent musk xylene (0.20 mg L^{-1}), these two compounds are still classified at the same toxicity level. A similar case was observed for the chronic toxicity of these transformation products in the aerated aquatic environment. That is, the chronically toxicity of the transformation products was reduced but they were still classified at the same toxicity level as parent musk xylene.

In summary, although all these transformation products exhibit a

decreased aquatic toxicity in comparison to the original musk xylene, they were still classified as toxic or very toxic. In particular, the cyclic products (PC1a and PC1b) and the demethylation product (PC2b) have a noticeable aquatic toxicity to fish. Thus, much attention should be paid to the aquatic toxicity of these transformation products, as well as musk xylene.

3.5. Carcinogenicity of musk xylene and its transformation products

Assessment of carcinogenic potential is considered a basic requirement when evaluating possible human health hazards related to chemical exposure. Previous research indicates that musk xylene has carcinogenic activity (Apostolidis et al., 2002). The carcinogenic potential of musk xylene and its transformation products was estimated (Table S6) to evaluate the carcinogenicity of the transformation products during the indirect photochemical process in aquatic environments and to explore whether or not they will have higher carcinogenic activity than original musk xylene. It is clear that the transformation products still have carcinogenic activity. In addition, the maximum recommended daily dose of musk xylene was determined as 0.02 mmol , while that of the $R_{abs}a$ pathway transformation product PC1a was estimated as only 0.01 mmol . This indicates that the carcinogenic activity of the transformation products from the cyclization pathway could be higher than the parent musk xylene. A similar result was observed in the $\cdot\text{OH}$ -rich aquatic environment. That is, the maximum recommended daily doses were determined as 0.02 and 0.01 mmol for

products MX-OH_a and PC2a, respectively. In the aerated aquatic environment, the transformation product PC3a, with a maximum recommended daily dose of 0.02 mmol, exhibited similar carcinogenic activity to parent musk xylene.

The maximum recommended daily dose for the transformation product PC1b from the *R*_{abs}b pathway was estimated as 0.02 mmol, indicating that the carcinogenic activity of the cyclization pathway transformation product could be the same as the parent musk xylene. A different case was seen under the ·OH-rich aquatic environment. That is, the maximum recommended daily doses were 0.02 mmol for product MX-OH_b and 0.04 mmol for product PC2b. This implies that although MX-OH_b has similar carcinogenic activity to parent musk xylene, further transformation to PC2b could decrease the carcinogenic activity. However, increased carcinogenic activity was observed in the aerated aquatic environment because the maximum recommended daily dose of the transformation product PC3b was 0.015 mmol.

In short, all products still have carcinogenic activity during ·OH-initiated transformation of musk xylene in aquatic environments. Increased carcinogenic activity was observed for the cyclic (PC1a) and aldehyde (PC2a and PC3b) products, relative to parent musk xylene. Based on the transformation mechanisms, the increased carcinogenicity resulted mainly from the transformation products of the H-abstraction pathway *R*_{abs}a, including the subsequent reaction of the cyclization pathway and the ·OH reaction. For the *R*_{abs}b pathway, the O₂ reaction could result in increased carcinogenic activity. Thus, these musk xylene transformation pathways in aquatic environments require much attention, and the potential risks resulting from these transformation products should be seriously evaluated.

4. Conclusions

The occurrence of synthetic musks, particularly the long-used nitro-musks, in aquatic environments has gained increasing attention due to their potential eco-toxicity and human health effects. To our knowledge, this is the first attempt at understanding indirect photochemical transformation of nitro-musks in aquatic environments using theoretical calculations. Both quantum chemistry and computational toxicology were employed to explore the transformation mechanisms, persistence and adverse effects on aquatic organisms and human health during the indirect photochemical process of a typical nitro-musk, namely musk xylene. We found that musk xylene was easily transformed at a rate constant of 5.65×10^8 – $8.79 \times 10^9 \text{ M}^{-1} \text{ s}^{-1}$. The main mechanism was proposed as an H-abstraction reaction from the methyl group of musk xylene, resulting in the formation of cyclic, aldehyde and demethylation products, as well as highly reactive ·OH. Although these transformation products exhibited a decreased aquatic toxicity, they still showed human carcinogenic activity. In particular, cyclic (PC1a) and aldehyde (PC2a and PC3b) products exhibited increased carcinogenic activity relative to parent musk xylene.

Acknowledgments

The authors appreciate the financial supports from National Natural Science Funds for Distinguished Young Scholars (41425015), National Natural Science Foundation of China (41603115), Leading Scientific, Technical and Innovation Talents of Guangdong Special Support Program (2016TX03Z094), The Innovation Team Project of Guangdong Provincial Department of Education (2017KCXTD012), National Natural Science Foundation of Guangdong, China (2016A030310120), and Science and Technology Program of Guangzhou, China (201804010128). In addition, we also want to thank the support from the National Supercomputer Center in Guangzhou.

Appendix A. Supplementary data

Supplementary data to this article can be found online at <https://>

doi.org/10.1016/j.envint.2019.05.020.

References

- Allen, J.M., Lucas, S., Allen, S.K., 1996. Formation of hydroxyl radical (·OH) in illuminated surface waters contaminated with acidic mine drainage. *Environ. Toxicol. Chem.* 15 (2), 107–113.
- An, T., Fang, H., Li, G., Wang, S., Yao, S., 2014. Experimental and theoretical insights into photochemical transformation kinetics and mechanisms of aqueous propylparaben and risk assessment of its degradation products. *Environ. Toxicol. Chem.* 33 (8), 1809–1816.
- Apostolidis, S., Chandra, T., Demirhan, I., Cinatl, J., Doerr, H.W., Chandra, A., 2002. Evaluation of carcinogenic potential of two nitro-musk derivatives, musk xylene and musk tibetene in a host-mediated in vivo/in vitro assay system. *Anticancer Res.* 22 (5), 2657–2662.
- Berset, J.D., Bigler, P., Herren, D., 2000. Analysis of nitro musk compounds and their amino metabolites in liquid sewage sludges using NMR and mass spectrometry. *Anal. Chem.* 72 (9), 2124–2131.
- Brezonik, P.L., Fulkerson-Brekken, J., 1998. Nitrate-induced photolysis in natural waters: controls on concentrations of hydroxyl radical photo-intermediates by natural scavenging agents. *Environ. Sci. Technol.* 32 (19), 3004–3010.
- Burns, J.M., Cooper, W.J., Ferry, J.L., King, D.W., DiMento, B.P., McNeill, K., Miller, C.J., Miller, W.L., Peake, B.M., Rusak, S.A., Rose, A.L., Waite, T.D., 2012. Methods for reactive oxygen species (ROS) detection in aqueous environments. *Aquat. Sci.* 74 (4), 683–734.
- Buth, J.M., Arnold, W.A., McNeill, K., 2007. Unexpected products and reaction mechanisms of the aqueous chlorination of cimetidine. *Environ. Sci. Technol.* 41 (17), 6228–6233.
- Butte, W., Schmidt, S., Schmidt, A., 1999. Photochemical degradation of nitrated musk compounds. *Chemosphere* 38 (6), 1287–1291.
- Canterino, M., Marotta, R., Temussi, F., Zarrelli, A., 2008. Photochemical behaviour of musk tibetene - a chemical and kinetic investigation. *Environ. Sci. Pollut. R.* 15 (3), 182–187.
- Chen, G.S., Jiang, R.F., Qiu, J.L., Cai, S.Y., Zhu, F., Ouyang, G.F., 2015. Environmental fates of synthetic musks in animal and plant: an in vivo study. *Chemosphere* 138, 584–591.
- ECOSAR, 2014. <http://www.epa.gov/oppt/newchems/tools/21ecosar.htm>.
- Fenner, K., Canonica, S., Wackett, L.P., Elsner, M., 2013. Evaluating pesticide degradation in the environment: blind spots and emerging opportunities. *Science* 341 (6147), 752–758.
- Frisch, M.J., Trucks, G.W., Schlegel, H.B., Scuseria, G.E., Robb, M.A., Cheeseman, J.R., Scalmani, G., Barone, V., Mennucci, B., Petersson, G.A., Nakatsuji, H., Caricato, M., Li, X., Hratchian, H.P., Izmaylov, A.F., Bloino, J., Zheng, G., Sonnenberg, J.L., Hada, M., Ehara, M., Toyota, K., Fukuda, R., Hasegawa, J., Ishida, M., Nakajima, T., Honda, Y., Kitao, O., Nakai, H., Vreven, T., Montgomery Jr., J.A., Peralta, J.E., Ogliaro, F., Bearpark, M.J., Heyd, J., Brothers, E.N., Kudin, K.N., Staroverov, V.N., Kobayashi, R., Normand, J., Raghavachari, K., Rendell, A.P., Burant, J.C., Iyengar, S.S., Tomasi, J., Cossi, M., Rega, N., Millam, N.J., Klene, M., Knox, J.E., Cross, J.B., Bakken, V., Adamo, C., Jaramillo, J., Gomperts, R., Stratmann, R.E., Yazyev, O., Austin, A.J., Cammi, R., Pomelli, C., Ochterski, J.W., Martin, R.L., Morokuma, K., Zakrzewski, V.G., Voth, G.A., Salvador, P., Dannenberg, J.J., Dapprich, S., Daniels, A.D., Farkas, Ö., Foresman, J.B., Ortiz, J.V., Cioslowski, J., Fox, D.J., 2009. Gaussian 09. Gaussian, Inc., Wallingford, CT, USA.
- Gao, Y., An, T., Fang, H., Ji, Y., Li, G., 2014a. Computational consideration on advanced oxidation degradation of phenolic preservative, methylparaben, in water: mechanisms, kinetics, and toxicity assessments. *J. Hazard. Mater.* 278 (0), 417–425.
- Gao, Y., Ji, Y., Li, G., An, T., 2014b. Mechanism, kinetics and toxicity assessment of OH-initiated transformation of triclosan in aquatic environments. *Water Res.* 49 (0), 360–370.
- Gao, Y., An, T., Ji, Y., Li, G., Zhao, C., 2015. Eco-toxicity and human estrogenic exposure risks from OH-initiated photochemical transformation of four phthalates in water: a computational study. *Environ. Pollut.* 206, 510–517.
- Gao, Y., Ji, Y., Li, G., An, T., 2016a. Theoretical investigation on the kinetics and mechanisms of hydroxyl radical-induced transformation of parabens and its consequences for toxicity: influence of alkyl-chain length. *Water Res.* 91, 77–85.
- Gao, Y., Ji, Y., Li, G., Mai, B., An, T., 2016b. Bioaccumulation and ecotoxicity increase during indirect photochemical transformation of polycyclic musk tonalide: a modeling study. *Water Res.* 105, 47–55.
- Gao, Y., Li, G., Ma, S., An, T., 2017. Research progress and challenge of synthetic musks: from personal care, environment pollution to human health. *Prog. Chem.* 29 (9), 1082–1092.
- Gao, L.W., Minakata, D., Wei, Z.S., Spinney, R., Dionysiou, D.D., Tang, C.J., Chai, L.Y., Xiao, R.Y., 2019. Mechanistic study on the role of soluble microbial products in sulfate radical-mediated degradation of pharmaceuticals. *Environ. Sci. Technol.* 53 (1), 342–353.
- Gatermann, R., Biselli, S., Huhnerfuss, H., Rimkus, G.G., Hecker, M., Karbe, L., 2002. Synthetic musks in the environment. Part 1: species-dependent bioaccumulation of polycyclic and nitro musk fragrances in freshwater fish and mussels. *Arch. Environ. Con. Tox.* 42 (4), 437–446.
- Hansel, R., Luh, L.M., Corbeski, I., Trantirek, L., Dotsch, V., 2014. In-cell NMR and EPR spectroscopy of biomacromolecules. *Angew. Chem. Int. Edit.* 53 (39), 10300–10314.
- Hopkins, Z.R., Blaney, L., 2016. An aggregate analysis of personal care products in the environment: identifying the distribution of environmentally-relevant concentrations. *Environ. Int.* 92–93, 301–316.
- Hutter, H.P., Wallner, P., Moshhammer, H., Hartl, W., Sattelberger, R., Lorbeer, G., Kundli,

- M., 2009. Synthetic musks in blood of healthy young adults: relationship to cosmetics use. *Sci. Total Environ.* 407 (17), 4821–4825.
- Hutter, H.P., Wallner, P., Hartl, W., Uhl, M., Lorbeer, G., Gminski, R., Mersch-Sundermann, V., Kundi, M., 2010. Higher blood concentrations of synthetic musks in women above fifty years than in younger women. *Int. J. Hyg. Environ. Heal.* 213 (2), 124–130.
- Janssen, E.M.L., Erickson, P.R., McNeill, K., 2014. Dual roles of dissolved organic matter as sensitizer and quencher in the photooxidation of tryptophan. *Environ. Sci. Technol.* 48 (9), 4916–4924.
- Kafferlein, H.U., Goen, T., Angerer, J., 1998. Musk xylene: analysis, occurrence, kinetics, and toxicology. *Crit. Rev. Toxicol.* 28 (5), 431–476.
- Kannan, K., Reiner, J.L., Yun, S.H., Perrotta, E.E., Tao, L., Johnson-Restrepo, B., Rodan, B.D., 2005. Polycyclic musk compounds in higher trophic level aquatic organisms and humans from the United States. *Chemosphere* 61 (5), 693–700.
- Karschuk, N., Tepe, Y., Gerlach, S., Pape, W., Wenck, H., Schmucker, R., Wittern, K.P., Schepky, A., Reuter, H., 2010. A novel in vitro method for the detection and characterization of photosensitizers. *PLoS One* 5 (12). <https://doi.org/10.1371/journal.pone.0015221>.
- Klasmeier, J., Matthies, M., Macleod, M., Fenner, K., Scheringer, M., Stroebe, M., Le Gall, A.C., McKone, T., Van De Meent, D., Wania, F., 2005. Application of multimedia models for screening assessment of long-range transport potential and overall persistence. *Environ. Sci. Technol.* 40 (1), 53–60.
- Lange, C., Kuch, B., Metzger, J.W., 2015. Occurrence and fate of synthetic musk fragrances in a small German river. *J. Hazard. Mater.* 282, 34–40.
- Li, C., Xie, H.B., Chen, J.W., Yang, X.H., Zhang, Y.F., Qiao, X.L., 2014. Predicting gaseous reaction rates of short chain chlorinated paraffins with $\cdot\text{OH}$: overcoming the difficulty in experimental determination. *Environ. Sci. Technol.* 48 (23), 13808–13816.
- Lignell, S., Darnerud, P.O., Aune, M., Cnattingius, S., Hajslova, J., Setkova, L., Glynn, A., 2008. Temporal trends of synthetic musk compounds in mother's milk and associations with personal use of perfumed products. *Environ. Sci. Technol.* 42 (17), 6743–6748.
- Liu, J.L., Wong, M.H., 2013. Pharmaceuticals and personal care products (PPCPs): a review on environmental contamination in China. *Environ. Int.* 59, 208–224.
- Luckenbach, T., Epel, D., 2005. Nitromusk and polycyclic musk compounds as long-term inhibitors of cellular xenobiotic defense systems mediated by multidrug transporters. *Environ. Health Persp.* 113 (1), 17–24.
- Luo, S., Gao, L.W., Wei, Z.S., Spinney, R., Dionysiou, D.D., Hu, W.P., Chai, L.Y., Xiao, R.Y., 2018. Kinetic and mechanistic aspects of hydroxyl radical-mediated degradation of naproxen and reaction intermediates. *Water Res.* 137, 233–241.
- Marenich, A.V., Cramer, C.J., Truhlar, D.G., 2009. Universal solvation model based on solute electron density and on a continuum model of the solvent defined by the bulk dielectric constant and atomic surface tensions. *J. Phys. Chem. B* 113 (18), 6378–6396.
- Maunz, A., Gutlein, M., Rautenberg, M., Vorgrimmler, D., Gebele, D., Helma, C., 2013. **lazar**: a modular predictive toxicology framework. *Front. Pharmacol.* 4. <https://doi.org/10.3389/fphar.2013.00038>.
- Nakata, H., Sasaki, H., Takemura, A., Yoshioka, M., Tanabe, S., Kannan, K., 2007. Bioaccumulation, temporal trend, and geographical distribution of synthetic musks in the marine environment. *Environ. Sci. Technol.* 41 (7), 2216–2222.
- Nakata, H., Hinosaka, M., Yanagimoto, H., 2015. Macrocyclic-, polycyclic-, and nitro musks in cosmetics, household commodities and indoor dusts collected from Japan: implications for their human exposure. *Ecotoxicol. Environ. Saf.* 111, 248–255.
- Neamtu, M., Siminiceanu, I., Kettrup, A., 2000. Kinetics of nitromusk compounds degradation in water by ultraviolet radiation and hydrogen peroxide. *Chemosphere* 40 (12), 1407–1410.
- Politzer, P., Lane, P., Jayasuriya, K., Domelsmith, L.N., 1987. Examination of some effects of NO_2 rotation in nitrobenzene. *J. Am. Chem. Soc.* 109 (7), 1899–1901.
- Ramirez, A.J., Brain, R.A., Usenko, S., Mottaleb, M.A., O'Donnell, J.G., Stahl, L.L., Wathen, J.B., Snyder, B.D., Pitt, J.L., Perez-Hurtado, P., Dobbins, L.L., Brooks, B.W., Chambliss, C.K., 2009. Occurrence of pharmaceuticals and personal care products in fish: results of a national pilot study in the United States. *Environ. Toxicol. Chem.* 28 (12), 2587–2597.
- Reiner, J.L., Wong, C.M., Arcaro, K.F., Kannan, K., 2007. Synthetic musk fragrances in human milk from the United States. *Environ. Sci. Technol.* 41 (11), 3815–3820.
- Rimkus, G.G., Gatermann, R., Huhnerfuss, H., 1999. Musk xylene and musk ketone amino metabolites in the aquatic environment. *Toxic. Lett.* 111 (1–2), 5–15.
- Salvito, D., 2005. Synthetic musk compounds and effects on human health? *Environ. Health Perspect.* 113 (12), A802–A803.
- Sanchez-Prado, L., Lores, M., Llompard, M., Garcia-Jares, C., Lourido, M., Cela, R., 2004. Further solid-phase microextraction-gas chromatography-mass spectrometry applications: “on-fibre” and aqueous photodegradation of nitro musks. *J. Chromatogr. A* 1048 (1), 73–80.
- Tas, J.W., Balk, F., Ford, R.A., van de Plassche, E.J., 1997. Environmental risk assessment of musk ketone and musk xylene in The Netherlands in accordance with the EU-TGD. *Chemosphere* 35 (12), 2973–3002.
- Wan, Y., Wei, Q.W., Hu, J.Y., Jin, X.H., Zhang, Z.B., Zhen, H.J., Liu, J.Y., 2007. Levels, tissue distribution, and age-related accumulation of synthetic musk fragrances in Chinese sturgeon (*Acipenser sinensis*): comparison to organochlorines. *Environ. Sci. Technol.* 41 (2), 424–430.
- Wang, Z., Chen, J., Sun, Q., Peijnenburg, W.J.G.M., 2011. C60-DOM interactions and effects on C60 apparent solubility: a molecular mechanics and density functional theory study. *Environ. Int.* 37 (6), 1078–1082.
- Xiao, R.Y., Ye, T.T., Wei, Z.S., Luo, S., Yang, Z.H., Spinney, R., 2015. Quantitative structure-activity relationship (QSAR) for the oxidation of trace organic contaminants by sulfate radical. *Environ. Sci. Technol.* 49 (22), 13394–13402.
- Xiao, R.Y., Luo, Z.H., Wei, Z.S., Luo, S., Spinney, R., Yang, W.C., Dionysiou, D.D., 2018. Activation of peroxymonosulfate/persulfate by nanomaterials for sulfate radical-based advanced oxidation technologies. *Curr. Opin. Chem. Eng.* 19, 51–58.
- Yamagishi, T., Miyazaki, T., Horii, S., Kaneko, S., 1981. Identification of musk xylene and musk ketone in freshwater fish collected from the Tama River, Tokyo. *Bull. Environ. Contam. Toxicol.* 26 (1), 656–662.
- Zeng, X.Y., Xu, L., Liu, J., Wu, Y., Yu, Z.Q., 2018. Occurrence and distribution of organophosphorus flame retardants/plasticizers and synthetic musks in sediments from source water in the Pearl River Delta, China. *Environ. Toxicol. Chem.* 37 (4), 975–982.
- Zhang, Y., Huang, L., Zhao, Y., Hu, T., 2017. Musk xylene induces malignant transformation of human liver cell line L02 via repressing the TGF-beta signaling pathway. *Chemosphere* 168, 1506–1514.
- Zhao, Y., Truhlar, D.G., 2008a. Density functionals with broad applicability in chemistry. *Acc. Chem. Res.* 41 (2), 157–167.
- Zhao, Y., Truhlar, D.G., 2008b. The M06 suite of density functionals for main group thermochemistry, thermochemical kinetics, noncovalent interactions, excited states, and transition elements: two new functionals and systematic testing of four M06-class functionals and 12 other functionals. *Theor. Chem. Accounts* 120 (1–3), 215–241.